Low-Temperature Heat Capacities of Potassium, Rubidium, and Cesium*

WILLIAM H. LIEN† AND NORMAN E. PHILLIPS‡
Department of Chemistry and Lawrence Radiation Laboratory, University of California, Berkeley, California
(Received 11 September 1963)

The heat capacities of potassium, rubidium, and cesium have been measured between 0.2 and 4.2°K. The thermal effective mass ratios are 1.25, 1.26, and 1.43, respectively. For potassium and rubidium these quantities are in reasonable agreement with theoretical estimates of the effects of band structure, electron-electron interactions, and electron-phonon interaction. The trends of the calculated and measured values suggest that the energy-band calculations overestimate the distortion of the Fermi surface in cesium. For potassium the elastic constants are known and can be compared with the observed T^3 term in the lattice heat capacity. The agreement is within the expected experimental errors. The T^5 term, however, does not agree with calculations based on a model that includes only first- and second-neighbor interactions.

I. INTRODUCTION

THEORETICAL studies of the electronic band structure of metals are most easily carried out for the alkalis, and as a consequence the band structure of these metals is relatively well understood. For these metals it would be of particular interest to compare the various measurable quantities determined by the band structure with one another and with the theoretical values. Such comparisons provide quantitative information about the effects of electron-electron and electron-phonon interactions if the band-theory calculations are assumed correct, and even without this assumption it is useful to compare the trends in the experimental quantities with those in the calculated values. One quantity of interest in this connection is the thermal effective mass m_t^* defined by

$$C_e=\gamma T \tag{1}$$

and

$$m_t^*/m_0=\gamma/\gamma_f, \tag{2}$$

where C_e is the electronic heat capacity, γ is a constant, T is the temperature, m_0 is the free electron mass, and γ_f is the value of γ for a gas of noninteracting electrons at the same density as the conduction electrons. For lithium and sodium, m_t^* can be obtained from measurements at liquid-helium temperatures and several experimental values are available for each.[1–6] For both of these metals, however, the interpretation of data is complicated by the existence of a Martensitic transformation[7] which produces a mixture of different crystal structures when the sample is cooled to the low temperatures necessary for the heat capacity measurements. Potassium, rubidium, and cesium do not undergo this transition, but heat capacity measurements below 1°K are required to separate the electronic heat capacity from that of the lattice. The measurements reported here permit this separation and an evaluation of m_t^*.

The measurements also give the low-temperature lattice heat capacity. This can be compared with the results of lattice dynamic calculations that have been most completely worked out for cubic structures. At low temperatures the lattice heat capacity C_l is given by

$$C_l=AT^3+BT^5+\cdots, \tag{3}$$

where A and B are constants characteristic of the material. The parameter A is equal to $(12/5)\pi^4R\theta_0^{-3}$, where θ_0 is the Debye characteristic temperature of the lattice at absolute zero. On the assumption that the low-energy thermal excitations are identical with sound waves, A and θ_0 are determined by the elastic constants. The T^5 term is largely produced by the excitation of modes of high enough frequency for dispersion to be important, and the coefficient B can be related to the elastic constants only through a model employing definite assumptions about the nature of the forces resisting displacement of the ion cores. It is the comparison of this term with experiment which provides the more stringent test of the lattice dynamic calculations.

For a metal, the heat capacity C is the sum of C_e and C_l. At sufficiently low temperatures experimental data can be represented by

$$C=\gamma T+AT^3 \tag{4}$$

or

$$C=\gamma T+AT^3+BT^5, \tag{5}$$

depending on the temperature range and the ratio B/A. For temperatures above the region of validity of Eq. (5), the lattice heat capacity is commonly represented by a temperature-dependent Debye characteristic temperature defined by equating $C-\gamma T$ to the Debye heat capacity function of T/θ.

* This work was supported by the U. S. Atomic Energy Commission. A preliminary report on some of this work has already been given in *Proceedings of the Seventh International Conference on Low Temperature Physics* (The University of Toronto Press, Toronto, 1960).

† Present address: Argonne National Laboratory, Argonne, Illinois.

‡ Alfred P. Sloan Research Fellow.

[1] L. M. Roberts, Proc. Phys. Soc. (London) **B70**, 744 (1957).
[2] D. L. Martin, Proc. Roy. Soc. (London) **A263**, 378 (1961).
[3] W. H. Lien and N. E. Phillips, Phys. Rev. **118**, 958 (1960).
[4] D. L. Martin, Phys. Rev. **124**, 438 (1961).
[5] R. E. Gaumer and C. V. Heer, Phys. Rev. **118**, 955 (1960).
[6] D. H. Parkinson and J. E. Quarrington, Proc. Phys. Soc. (London) **A68**, 762 (1955).
[7] C. S. Barrett, Acta Cryst. **9**, 671 (1956).

II. APPARATUS AND SAMPLES

The data for each sample were obtained in two separate experiments covering the temperature ranges of approximately 0.2 to 1.2°K and 1.2 to 4.2°K. For each sample there is an interval of 0.1 or 0.2°K in which the two experiments overlap.

The experimental procedures differ from those described in connection with other measurements[8] in only two significant respects. First, the nature of the samples required that they be enclosed in a sealed calorimeter and therefore the heater and thermometer could not be attached directly to the sample. The consequences of this modification are discussed later. Secondly, for the measurements in the adiabatic demagnetization region, temperature measurements were based on a different extrapolation (from above 1°K) of the susceptibility of copper potassium sulfate: the mutual inductance of coils surrounding the salt was taken to be inversely proportional to $(T-0.042)$. Experience with a number of metals for which the heat capacity at a few tenths of a degree can be predicted from other measurements shows that heat capacities based on this extrapolation are accurate to within about 1% in the temperature region reported here.[9]

The samples were obtained from commercial sources and were of stated purity 99.99, 99.8, and 99.8% for the potassium, rubidium, and cesium, respectively. The potassium sample used in earlier measurements[3] was from the same source. The range of temperatures over which the cesium sample melted suggested that the suppliers had overestimated the purity and therefore several different samples of similar stated purity were obtained. Analyses showed that all the samples had impurity contents that were comparable to each other but appreciably in excess of that stated by the suppliers. The potassium and rubidium samples, on which the heat capacity measurements were already complete, were also analyzed. The analysis indicated the following impurity contents: in the potassium sample, 0.2% sodium; in the rubidium sample, 3% potassium and 0.1% cesium; in the cesium sample, 0.2% sodium, 0.2% potassium, and 0.4% rubidium. No other impurities were detected spectroscopically. As discussed in a later section, these impurities are unlikely to affect the electronic heat capacity by more than the experimental error. The effect on the lattice heat capacity is difficult to estimate, but the similarity in the properties of the alkalis suggests that it is not large.

The body of each calorimeter and its cap were machined from solid copper rods. The cap included a vane that extended into the interior of the calorimeter to improve thermal contact with the sample. The samples were cast into the calorimeters and the calorimeters sealed with solder in a single operation carried out under an argon atmosphere. The thermal link to the superconducting heat switch and the cooling salt was silver soldered to the surface of the calorimeter. The thermometer and heater were attached with varnish. The heat capacity of each calorimeter was calculated from the heat capacities of the materials used. The heat capacity of one calorimeter was measured and found to be in good agreement with the estimated heat capacity.

The heat capacity of the empty calorimeter—and hence the correction to the total measured heat capacity—was in each case greatest at the lowest temperatures. At 0.2°K the empty calorimeters accounted for 30, 36, and 39% of the total heat capacity in the potassium, rubidium, and cesium experiments, respectively. Above 1°K the corrections were not large enough to affect significantly the accuracy of the final results.

[8] N. E. Phillips, Phys. Rev. 114, 676 (1959).
[9] N. E. Phillips (to be published).

TABLE I. The heat capacity of potassium: measurements in the adiabatic demagnetization cryostat. The units of heat capacity are mJ mole^{-1} deg^{-1}. Temperatures are based on the 1958 He^4 scale.[a]

T	C	T	C	T	C
0.2604	0.5852	0.3644	0.8858	0.7697	2.798
0.2781	0.6306	0.3935	0.9733	0.8296	3.242
0.2953	0.6786	0.4231	1.021	0.8922	3.765
0.2501	0.5592	0.4515	1.177	0.7236	2.511
0.2698	0.6066	0.4835	1.302	0.7785	2.877
0.2894	0.6657	0.4969	1.353	0.8332	3.310
0.3067	0.7104	0.5435	1.551	0.8902	3.757
0.3270	0.7687	0.5944	1.786	0.8710	3.617
0.3478	0.8362	0.6414	2.027	0.9334	4.083
0.3734	0.9180	0.6901	2.303	1.013	4.899
0.3994	1.003	0.4805	1.292	1.101	5.884
0.4274	1.102	0.5259	1.471	1.180	6.874
0.4578	1.208	0.5661	1.659	1.218	7.390
0.2650	0.5969	0.6122	1.882	1.238	7.696
0.2885	0.6578	0.6614	2.143		
0.3379	0.7962	0.7155	2.458		

[a] See Ref. 10.

TABLE II. The heat capacity of potassium: measurements in the liquid-helium temperature cryostat. The units of heat capacity are mJ mole^{-1} deg^{-1}. Temperatures are based on the 1958 He^4 scale.[a]

T	C	T	C	T	C
1.1606	6.519	2.9140	79.98	1.9358	24.00
1.2392	7.585	3.1103	98.09	2.0585	28.47
1.3243	8.898	3.3140	119.9	2.1932	34.11
1.4162	10.49	3.5308	146.4	2.3415	41.30
1.5274	12.75	3.7669	179.5	2.5007	50.26
1.6458	15.50	4.0309	223.1	2.6600	60.48
1.7582	18.40	1.1421	6.278	2.8279	73.27
1.8741	21.90	1.2033	7.115	3.0084	88.62
1.9978	26.14	1.2834	8.269	3.2078	108.6
2.1300	31.36	1.3918	10.07	3.4143	132.1
2.2725	37.81	1.4897	11.97	3.6325	160.6
2.4205	45.44	1.5884	14.12	3.8819	198.1
2.5738	54.67	1.6968	16.80	4.1012	236.2
2.7357	65.88	1.8162	20.15		

[a] See Ref. 10.

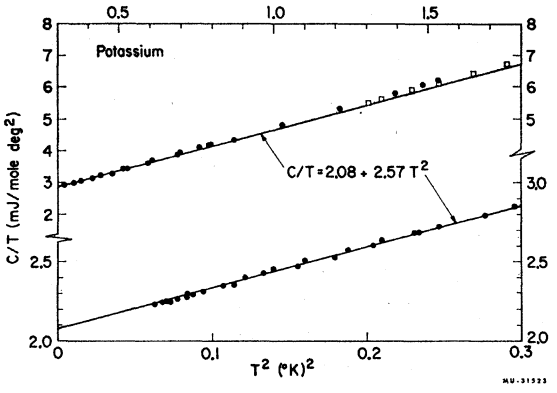

FIG. 1. C/T versus T^2 for potassium. □: liquid-helium cryostat; ●: adiabatic demagnetization cryostat.

III. EXPERIMENTAL RESULTS

The heat capacity points obtained in the six experiments are presented in Tables I to VI.

If the experimental heat capacity points were all of equal accuracy the best method of analysis of the data would be to plot C/T versus T^2 and to find γ and A of Eq. (4) from the intercept and limiting slope at $T^2=0$. In this work the measurements above 1°K are expected to be appreciably more accurate than those below 1°K, and it is therefore appropriate to give some weight to the points above 1°K even in the determination of γ. This can be done through the requirement that Eq. (5) represents the data at temperatures at which deviations from Eq. (4) first became important. This requirement can have an appreciable affect on the assignment of values of γ and A.

There is a further complication in the analysis of these experiments. The experimental points for potassium and cesium taken in the adiabatic demagnetization cryostat and those taken in the liquid-helium cryostat do not join smoothly in the region of overlap. In each case the points obtained in the adiabatic demagnetization cryostat are high. The discrepancy in heat capacity at 1.2°K, after the heat capacity of the empty calorimeter is subtracted, is 1.3% for potassium and 3% for cesium, as will be seen in Figs. 1 and 3. This discrepancy has not been observed in other experiments in this apparatus, and is apparently associated with the fact that in these experiments heat is introduced to the surface of the calorimeter instead of directly to the sample. This produces a superheating of the calorimeter during the heating periods, with the consequence that the heat loss from the calorimeter to the surroundings during the heating period is greater than that estimated from the drift rates before and after the heating period. This effect is not important in

TABLE III. The heat capacity of rubidium: measurements in the adiabatic demagnetization cryostat. The units of heat capacity are mJ mole^{-1} deg^{-1}. Temperatures are based on the 1958 He^4 scale.[a]

T	C	T	C	T	C
0.2002	0.5701	0.2548	0.8022	0.5867	3.810
0.2191	0.6439	0.2798	0.9257	0.6418	4.724
0.2391	0.7282	0.3048	1.063	0.7053	5.924
0.2616	0.8336	0.3285	1.201	0.7736	7.457
0.2936	0.9953	0.3511	1.350	0.8497	9.489
0.1954	0.5537	0.3830	1.582	0.9289	11.87
0.2143	0.6223	0.4177	1.863	1.011	14.93
0.2321	0.6968	0.4527	2.172	1.098	18.85
0.2548	0.8001	0.4882	2.538	0.6381	4.617
0.2819	0.9344	0.5252	2.979	0.7084	5.947
0.3140	1.113	0.5686	3.555	0.7862	7.735
0.3456	1.309	0.6151	4.229	0.8634	9.845
0.3816	1.569	0.6573	4.931	0.9455	12.49
0.4185	1.868	0.7245	6.264	1.041	16.26
0.4615	2.260	0.7969	7.952	1.135	20.71
0.5015	2.693	0.8708	10.02	1.237	26.43
0.5549	3.358	0.4168	1.860	1.214	25.13
0.1859	0.5189	0.4596	2.255	1.167	22.46
0.2087	0.6064	0.5002	2.681	1.245	26.88
0.2326	0.7025	0.5395	3.121		

[a] See Ref. 10.

TABLE IV. The heat capacity of rubidium: measurements in the liquid-helium temperature cryostat. The units of heat capacity are mJ mole^{-1} deg^{-1}. Temperatures are based on the 1958 He^4 scale.[a]

T	C	T	C	T	C
1.1991	24.07	4.0713	1009.	3.6579	757.7
1.3249	32.22	1.1952	23.83	4.0081	969.1
1.4630	43.46	1.3076	30.99	1.5881	55.89
1.6163	59.22	1.4365	41.12	1.7361	73.97
1.7867	81.31	1.5882	56.00	1.9055	99.58
1.9718	111.4	1.7523	76.35	2.0910	134.4
2.1610	149.7	1.9314	104.3	2.2887	179.3
2.3660	200.3	2.1287	142.6	2.5015	238.5
2.5961	269.1	2.3342	191.4	2.7254	313.0
2.8521	361.7	2.5471	251.8	2.9798	412.5
3.1428	486.5	2.7886	336.9	3.2642	543.7
3.4535	644.5	3.0530	445.1	3.5784	711.6
3.7762	827.6	3.3361	581.4	3.9231	914.7

[a] See Ref. 10.

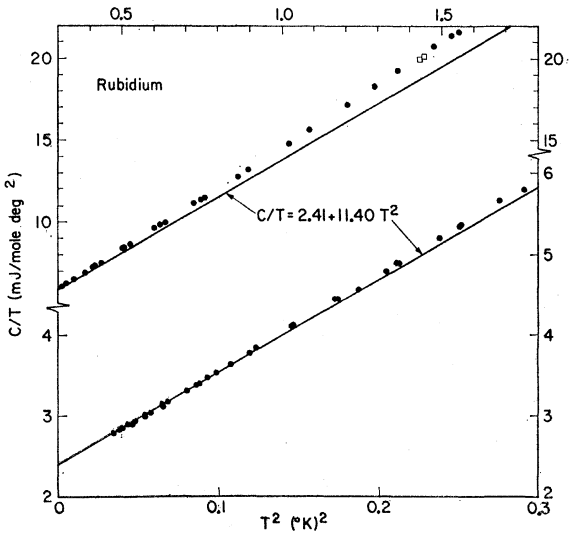

FIG. 2. C/T versus T^2 for rubidium. □: liquid-helium cryostat; ●: adiabatic demagnetization cryostat.

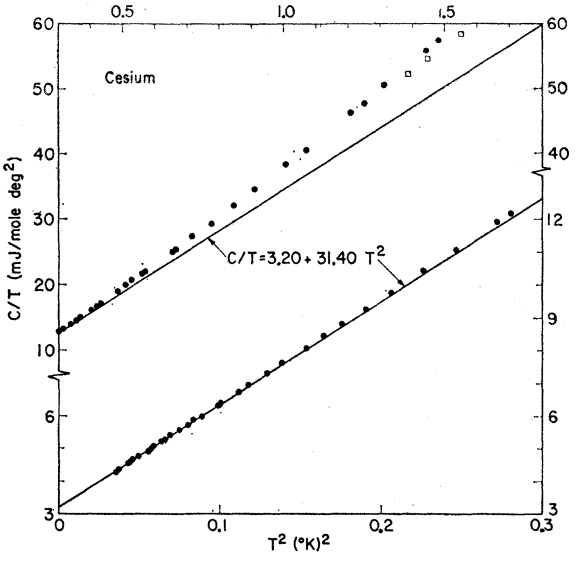

FIG. 3. C/T versus T^2 for cesium. □: liquid-helium cryostat; ●: adiabatic demagnetization cryostat.

the experiments in the liquid-helium cryostat because the thermal isolation of the sample is always good in those experiments, nor is it important at the lowest temperatures in the adiabatic demagnetization cryostat, for the same reason. However, it does become important near 1°K in the adiabatic demagnetization apparatus because the thermal conductivity of the superconducting link to the cooling salt increases very rapidly with temperature. Proof that the effect is not important at the very low temperatures or in the experiments in the liquid-helium region is that in those experiments no systematic differences were observed between heat capacity points taken with different heater powers at the same temperature. This interpretation of the discontinuity at 1.2°K is supported by a strong correlation between the thermal resistance of the superconducting switch and the size of the discontinuity. The rate of temperature drift between heating periods in the adiabatic demagnetization experiments depends on the dimensions of the superconducting link, and was greatest in the cesium experiment and least in the rubidium experiment. This shows that the order of decreasing thermal isolation is the same as the order of increasing discrepancy. Further support for this interpretation is the possibility of finding values of γ, A, and B such that Eq. (5) provides a reasonable fit to the lowest points taken at liquid-helium temperatures and also to points taken below about 0.7°K in the adiabatic demagnetization cryostat. This will be seen most clearly in Fig. 6.

Values of γ, A, and B were obtained in the following way. First a plot of C/T versus T^2, using points from the below 1°K experiments, was used to determine a preliminary value of γ. These points are shown in

TABLE V. The heat capacity of cesium: measurements in the adiabatic demagnetization cryostat. The units of heat capacity are mJ mole^{-1} deg^{-1}. Temperatures are based on the 1958 He^4 scale.[a]

T	C	T	C	T	C
0.1874	0.8048	0.6550	11.29	0.8072	20.20
0.2073	0.9445	0.7130	14.24	0.8801	25.82
0.2351	1.159	0.2080	0.9499	0.9524	32.96
0.2568	1.357	0.2225	1.061	1.034	41.98
0.2832	1.624	0.2361	1.177	1.118	53.35
0.3143	1.988	0.2519	1.313	1.217	69.85
0.1923	0.8402	0.2739	1.524	1.146	57.92
0.2141	1.003	0.2984	1.786	1.099	50.97
0.2416	1.226	0.3155	1.996	1.200	66.98
0.2629	1.428	0.3339	2.247	1.002	38.42
0.2883	1.691	0.3598	2.629	0.5293	6.451
0.3166	2.031	0.3916	3.158	0.5800	8.147
0.3434	2.390	0.4190	3.695	0.6321	10.26
0.3719	2.833	0.4539	4.433	0.6884	12.93
0.4056	3.431	0.4963	5.490	0.7503	16.43
0.4370	4.051	0.5480	7.035	0.8136	20.64
0.4755	4.964	0.5952	8.728	0.8457	23.10
0.5214	6.210	0.6461	10.87	0.9181	29.45
0.5612	7.474	0.6951	13.31		
0.6059	9.156	0.7468	16.19		

[a] See Ref. 10.

TABLE VI. The heat capacity of cesium: measurements in the liquid-helium temperature cryostat. The units of heat capacity are mJ mole^{-1} deg^{-1}. Temperatures are based on the 1958 He^4 scale.[a]

T	C	T	C	T	C
1.2031	65.61	3.0238	1077.	2.0522	351.8
1.2932	82.03	3.2512	1299.	2.2053	439.2
1.3883	102.8	3.5012	1566.	2.3645	541.2
1.4897	128.8	3.7667	1861.	2.5355	662.7
1.6006	161.6	4.0437	2180.	2.7183	805.4
1.7185	202.8	1.1779	61.56	2.9183	978.2
1.8435	253.2	1.2459	73.14	3.1364	1185.
1.9803	317.3	1.3371	91.29	3.3691	1421.
2.1302	397.5	1.4374	114.7	3.6290	1702.
2.2875	492.0	1.5444	144.1	3.8761	1978.
2.4529	605.4	1.6575	180.2	4.0880	2217.
2.6285	735.7	1.7799	226.0		
2.8182	892.4	1.9111	282.1		

[a] See Ref. 10.

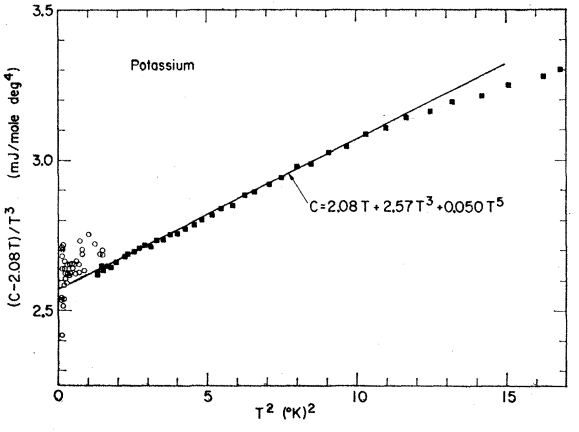

FIG. 4. The lattice heat capacity of potassium. ■: liquid-helium cryostat; ○: adiabatic demagnetization cryostat.

TABLE VII. The coefficients γ, A, and B in the expression $C=\gamma T+AT^3+BT^5$.

Metal	γ (mJ mole^{-1} deg^{-2})	A (mJ mole^{-1} deg^{-4})	B (mJ mole^{-1} deg^{-6})
K	2.08±0.03	2.57±0.05	0.050±0.003
Rb	2.41±0.04	11.40±0.1	0.636±0.05
Cs	3.20±0.07	31.40±0.2	2.78 ±0.2

Figs. 1, 2, and 3 together with straight lines corresponding to the values of γ and A finally adopted. The preliminary values of γ together with values 1 and 2% higher and lower were used to construct graphs of $(C-\gamma T)/T^3$ versus T^2. These graphs were used as a guide in selecting the final values of γ, and A and B were then taken as the intercept and slope at $T^2=0$. This second step in the analysis did not change the preliminary γ value for cesium, but increased it by 1.0% for potassium and 1.7% for rubidium. The comparison of the data with Eq. (5) is shown in Figs. 4, 5, and 6. The values of γ, A, and B are given in Table VII.

On the basis of past experience with the apparatus the precision expected is within a few tenths of a percent at liquid-helium temperatures and about 1% in the adiabatic demagnetization region. These figures also apply to the total measured heat capacity in the experiments reported here. The accuracy is more difficult to estimate. Except for points above 0.7°K taken in the adiabatic demagnetization cryostat, it is limited by errors in temperature measurement, including possible errors in the helium vapor-pressure scale, the vapor-pressure measurements, and the extrapolation of readings of the mutual inductance bridge to below 1°K. The resulting error in the heat capacity of the sample seems likely to be no more than 0.3% at liquid-helium temperatures, 1% down to 0.3°K, and 1.5% at 0.2°K. The limits of error

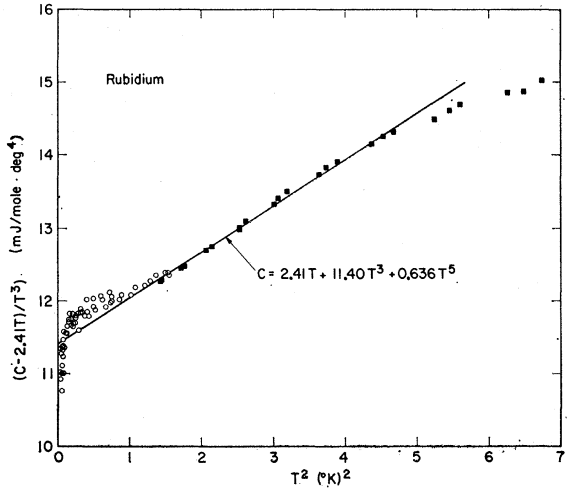

FIG. 5. The lattice heat capacity of rubidium. ■: liquid-helium cryostat; ○: adiabatic demagnetization cryostat.

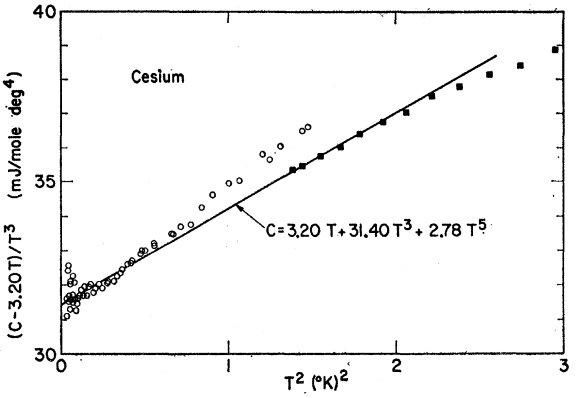

FIG. 6. The lattice heat capacity of cesium. ■: liquid-helium cryostat; ○: adiabatic demagnetization cryostat.

indicated in Table VII represent qualitative estimates based on these figures and intended to take into account the uncertainties in the analysis of the data described above.

Potassium, rubidium, and cesium, unlike lithium and sodium, can be expected to have heat capacities which are independent of sample treatment. The experimental data in the liquid-helium region are summarized in Table VIII. Since the other work does not go to low enough temperatures to permit an analysis of the data into electronic and lattice heat capacities, comparison is made on the basis of total heat capacity. The potassium measurements agree well with those by Roberts,[1] except at 1.5°K, where Roberts' values include a correction for effects of helium exchange gas which could very well account for the discrepancy. In some cases the disagreement with the other measurements on rubidium and cesium may exceed the combined experimental errors, although disagreement of this magnitude is not without precedent at these temperatures. Neither McCollum and Silsbee[11] nor Manchester[12] give analyses of their samples, but these were

TABLE VIII. Comparison of experimental data with other work in the liquid-helium region.

Metal	C (mJ mole^{-1} deg^{-1}) 1.5°K	2.0°K	3.0°K	4.0°K	Reference
K	12.2	26.3	87.8	218	This work.
K	12.7	26.4	86.6	215	L. M. Roberts.[a]
Rb	47	117	423	963	This work.
Rb	48	120	440	972	McCollum and Silsbee.[b]
Rb	46	107	391	898	F. D. Manchester.[c]
Cs	131	326	1054	2124	This work.
Cs	129	310	990	1980	McCollum and Silsbee.[b]

[a] See Ref. 1.
[b] See Ref. 11.
[c] See Ref. 12.

[10] F. G. Brickwedde, H. van Dijk, M. Durieux, J. R. Clement, and J. K. Logan, J. Res. Natl. Bur. Std. (U. S.) 64A, 1 (1960).
[11] D. C. McCollum, Jr., and H. B. Silsbee, Phys. Rev. 127, 119 (1962).
[12] F. D. Manchester, Can. J. Phys. 37, 525 (1959).

TABLE IX. Comparison of effective mass ratios with theoretical predictions.

	K	Rb	Cs
1. γ (mJ mole^{-1} deg^{-2})	2.08 ±0.03	2.41 ±0.04	3.20 ±0.07
2. γ_f (mJ mole^{-1} deg^{-2})[a]	1.669	1.907	2.233
3. $m_t^*/m_0=\gamma/\gamma_f$	1.25 ±0.02	1.26 ±0.02	1.43 ±0.03
4. m_t^*/m_0 (Band-theory calculation)[b]	1.09	1.21	1.76
5. m^*/m_0 (Band-theory calculation)[c]	0.86	0.78	0.73
6. m^*/m_0 (Electron-electron interactions)[d]	0.93	0.95	0.96
7. m^*/m_0 (Electron-phonon interactions)[e]	1.26	1.40	1.51
8. m^*/m_0 (Electron-phonon interactions)[f]	1.59	1.61	1.69

[a] The lattice constants determined by Barrett at 5°K (Ref. 7) were used to calculate the atomic volume.
[b] See Ref. 14. The calculations employ the quantum defect method to obtain the energy as a function of wave number for certain directions in wave-number space together with an interpolation procedure to obtain the density of states.
[c] See Ref. 13. m^* is the effective mass at the bottom of the band.
[d] See Ref. 15.
[e] Calculated from the theory of Buckingham and Schafroth (Ref. 16).
[f] See Ref. 17.

obtained commercially and are likely to have impurity contents similar to those of the present samples. If the discrepancies in Table VIII are attributed to differing sample purity it follows that the θ values reported below may be affected by impurities by as much as 2% at the higher temperatures.

IV. DISCUSSION

Electronic Heat Capacity

The experimental m_t^*/m_0 ratios are compared with the results of some of the pertinent theoretical work in Table IX. The theoretical studies treat separately the effects of the periodic potential of the lattice[13,14] (rows 4 and 5), electron-electron interactions[15] (row 6), and electron-phonon interactions[16,17] (rows 7 and 8).

It is possible to compare the m_t^*/m_0 ratio for potassium directly with other experiments. Cyclotron resonance experiments by Grimes and Kip[18] show that the Fermi surface is spherical to within 1% and give an effective mass ratio of 1.21±0.02, in agreement with the value obtained in this work, 1.25±0.02. Thorsen and Berlincourt[19] have obtained an effective mass ratio of 0.90±0.09 from the de Haas-van Alphen effect. In the absence of interactions all three of these effective mass ratios should be the same for a metal with a spherical Fermi surface. The observed values suggest that the interactions contribute to the cyclotron mass and the thermal mass in the same way but to the amplitude of the de Haas-van Alphen oscillations in a different way.

If it is assumed that the various contributions to the deviation of the effective mass ratio from unity can be treated independently and that Ham's energy-band calculations (row 4 of Table IX) are correct, the difference between rows 3 and 4 shows that the combined effect of interactions is to increase the effective mass in potassium by about 15%. In fact, the cyclotron resonance experiments show that Ham's calculations overestimate the distortion of the Fermi surface and therefore probably overestimate the density of states, so that the effect of interactions is likely to be somewhat greater than 15%. In view of the difficulty associated with quantitative treatment of the interactions this must be considered as reasonable agreement with theoretical predictions for potassium.

As shown in Table IX, the theoretical treatment of interactions predicts an increasing m^* in the sequence potassium, rubidium, cesium, whereas the experimental m_t^*/m_0 decreases relative to the band-theory value. For rubidium the discrepance between these trends is perhaps not significant, but for cesium the calculated effect of interactions would have to have the wrong sign if the energy-band calculations are correct. Ham's calculations for cesium give a highly distorted Fermi surface which is close to contact with the zone boundary. The density of states is near a maximum and would be reduced by either a decrease in the amount of distortion of the Fermi surface or the slight increase necessary to produce contact. A change in either direction in the estimated distortion of the Fermi surface could therefore resolve the discrepancy. A qualitative

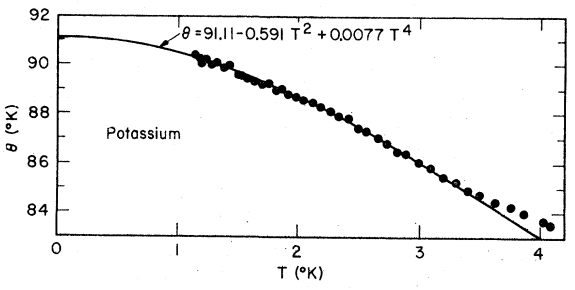

FIG. 7. θ versus T for potassium. At low temperatures the curve is equivalent to the straight line of Fig. 4.

[13] F. S. Ham, Phys. Rev. 128, 82 (1962).
[14] F. S. Ham, Phys. Rev. 128, 2524 (1962).
[15] D. Pines, in *Solid State Physics*, edited by F. Seitz and D. Turnbull (Academic Press Inc., New York, 1955), Vol. 1, p. 367.
[16] M. J. Buckingham and M. R. Schafroth, Proc. Phys. Soc. (London) A67, 828 (1954).
[17] J. J. Quinn, in *The Fermi Surface*, edited by W. A. Harrison and M. B. Webb (John Wiley & Sons, Inc., New York, 1960), p. 63.
[18] C. C. Grimes and A. F. Kip (to be published).
[19] A. C. Thorsen and T. G. Berlincourt, Phys. Rev. Letters 6, 617 (1961).

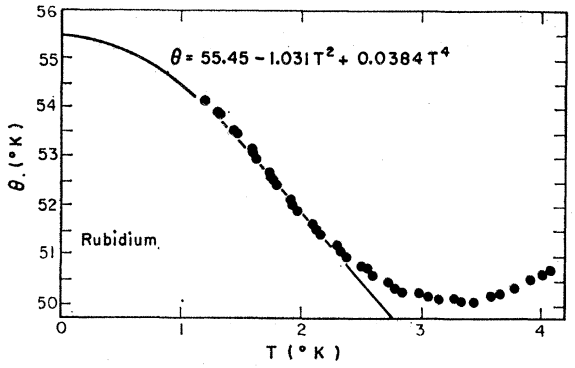

FIG. 8. θ versus T for rubidium. At low temperatures the curve is equivalent to the straight line of Fig. 5.

argument by Cohen and Heine[20] suggests that calculations of the type carried out by Ham overestimate the distortion of the Fermi surface by an amount which increases in the sequence potassium, rubidium, cesium. As noted by Ham,[14] this could be the reason for the poor agreement between theory and experiment for cesium. The cyclotron resonance experiment of Grimes and Kip[18] supports this interpretation by demonstrating that the energy-band calculations do overestimate the distortion of the Fermi surface for potassium.

In summary, there is reasonable agreement between the experimental m_i^*/m_0 and the various theoretical calculations for potassium, but for the heavier alkali metals it appears likely that the distortion of the Fermi surface is exaggerated by the energy-band calculations.

The presence of appreciable amounts of other alkali metals in the samples raises the question of the extent to which the experimental m_i^*/m_0 values are influenced by the purity of the sample. A convenient basis for discussion of this point is provided by the model devised by Cohen and Heine[20] to interpret the properties of the monovalent metals and the α-phase alloys of the noble metals. In this model the effective mass at the bottom of the band m^* is related to the atomic volume and to the energy gap at the centers of those faces of the first Brillouin zone nearest the center of the zone. The energy gap is in turn related to the difference in energy of atomic s and p states, Δ_{sp}. If the Fermi surface does not contact the zone boundary alloying will have similar effects on m^* and on m_i^*. In the present case the only significant effect of alloying is to modify the energy gap at the zone face. The assumption that this is determined by an average of Δ_{sp} for the different atoms leads to the conclusion that the effect of the impurity content on γ is less than the estimated experimental error.

Lattice Heat Capacity

The lattice heat capacities of potassium, rubidium, and cesium are shown in Figs. 7, 8, and 9 as plots of θ versus T. Beattie's table[21] of the Debye heat capacity function was used to calculate θ for the individual heat capacity points in the liquid-helium region. In addition, extrapolations to $T=0$ are given which are equivalent to the straight lines in Figs. 4, 5, and 6. Figure 10 shows smooth curves of θ/θ_0 versus T/θ_0 for potassium, rubidium, and cesium, together with smoothed points obtained by other workers at higher temperatures.

TABLE X. Comparison of the T^3 and T^5 terms in the lattice heat capacity derived from this work, with de Launay's results.

Metal	A (mJ mole^{-1} deg^{-4})	θ_0 (°K)	B (mJ mole^{-1} deg^{-6})	f'	
K	2.57	91.1	0.050	178	This work.
K	2.44	92.7	0.026	92	de Launay.[a]
Rb	11.40	55.5	0.636	172	This work.
Rb	14.44	51.3	0.577	105	de Launay.[a]
Cs	31.40	39.5	2.78	142	This work.
Cs	33.81	38.6	2.33	103	de Launay.[a]

[a] See Ref. 22.

De Launay[22] has given expressions for the T^3 and T^5 terms in the lattice heat capacity for cubic metals. The model used assumed central forces between first and second neighbors, and a volume force representing the contribution of the conduction electrons. The three parameters introduced are determined in terms of the independent elastic constants for cubic crystals, and tables are given permitting evaluation of the coefficients A and B in Eq. (2) in terms of these constants. De Launay distinguishes two cases: Case I, in which the contribution of the electrons to the elastic constants is assumed not to contribute to the restoring forces involved in thermal excitation, and Case II, in which it is assumed that the electrons do contribute. The heat capacity calculated in the two cases is not very different, presumably because the longitudinal vibrations, the only ones affected by the bulk modulus of the electron gas, make only a minor contribution to the low-temperature heat capacity. Experimental data suggest that for the lowest frequency modes, which

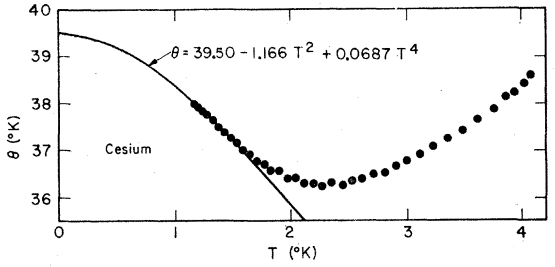

FIG. 9. θ versus T for cesium. At low temperatures the curve is equivalent to the straight line of Fig. 6.

[20] M. H. Cohen and V. Heine, Advan. Phys. 7, 396 (1958).

[21] J. A. Beattie, J. Math. & Phys. 6, 1 (1926).

[22] J. de Launay, in *Solid State Physics*, edited by F. Seitz and D. Turnbull (Academic Press Inc., New York, 1956), Vol. 2, pp. 219–303.

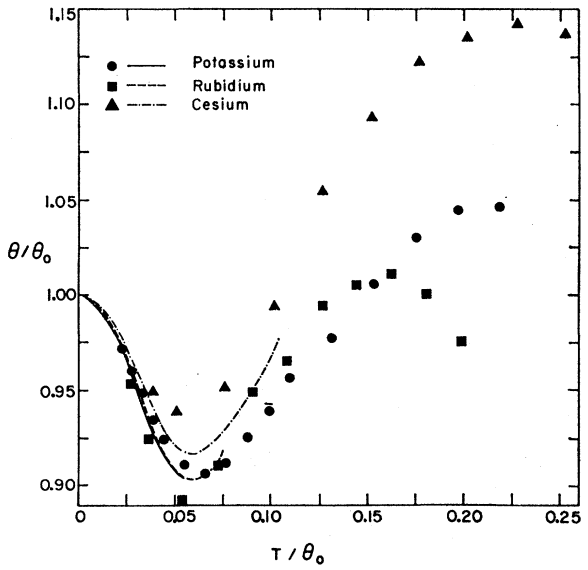

FIG. 10. θ/θ_0 versus T/θ_0 for potassium, rubidium, and cesium. ●: calculated from the data of Roberts (Ref. 1); ■, ▲: from the data of McCollum and Silsbee (Ref. 11).

determine the T^3 term, the electrons must follow the motion of the ions, and therefore Case II must apply.[22] This leads to the same relation between θ_0 and the elastic constants as in the Debye theory, and the agreement generally found between calorimetric and elastic constants data cannot be taken as supporting the other details of the model. The coefficients of the T^3 and T^5 terms in the lattice heat capacity are compared with de Launay's calculations in Table X. Only approximate values of the elastic constants are available for potassium, rubidium, and cesium, and the ones used in the comparison were taken from the compilation by Huntington.[23] In this table, f' is a parameter introduced by de Launay and is given by

$$C_l = (12/5)\pi^4 R[(T/\theta_0)^3 + f'(T/\theta_0)^5]. \quad (6)$$

The discrepancy between the calorimetric and elastic-constants data for the θ_0's of rubidium and cesium is probably largely due to the uncertainty in the calculated elastic constants. The elastic constants of potassium were measured at 77°K and extrapolated to 0°K, and the agreement is reasonable.

The observed coefficient of the T^5 term is in poor agreement with theory. For potassium, the comparison is clear. The elastic constants are relatively well known and predict θ_0 with reasonable accuracy, but there is a disagreement by a factor of two between the calculated and experimental B or f'. For rubidium and cesium the uncertainty in the elastic constants makes the comparison less clear, but there seems to be significant disagreement. The difference between the calculated and observed T^5 terms is probably caused by the inadequacy of a model that includes only second-neighbor interactions.

[23] H. B. Huntington, in *Solid State Physics*, edited by F. Seitz and D. Turnbull (Academic Press Inc., New York, 1958), Vol. 7, p. 288.